

See discussions, stats, and author profiles for this publication at: <https://www.researchgate.net/publication/283780212>

Hybrid-Functional Calculations on the Incorporation of Na and K Impurities Into the CuInSe_2 and $\text{CuIn}_{5/8}\text{Se}_8$ Solar Cell Materials

ARTICLE in THE JOURNAL OF PHYSICAL CHEMISTRY C · OCTOBER 2015

Impact Factor: 4.77 · DOI: 10.1021/acs.jpcc.5b07639

READS

80

8 AUTHORS, INCLUDING:



Hossein Mirhosseini

Max Planck Institute for Chemical Physics of S...

24 PUBLICATIONS 176 CITATIONS

SEE PROFILE



Guido Roma

Atomic Energy and Alternative Energies Com...

42 PUBLICATIONS 354 CITATIONS

SEE PROFILE



Thomas D Kühne

Universität Paderborn

64 PUBLICATIONS 1,142 CITATIONS

SEE PROFILE



Claudia Felser

Max Planck Institute for Chemical Physics of S...

535 PUBLICATIONS 8,522 CITATIONS

SEE PROFILE

Hybrid-Functional Calculations on the Incorporation of Na and K Impurities into the CuInSe_2 and CuIn_5Se_8 Solar-Cell Materials

Elaheh Ghorbani,^{†,‡} Janos Kiss,[§] Hossein Mirhosseini,^{*,§} Guido Roma,^{||,†} Markus Schmidt,[‡] Johannes Windeln,[⊥] Thomas D. Kühne,[▽] and Claudia Felser[§]

[†]Institute of Inorganic and Analytical Chemistry, Johannes Gutenberg University of Mainz, Staudinger Weg 9, 55122 Mainz, Germany

[‡]IBM, Hechtsheimer Straße 2, 55131 Mainz, Germany

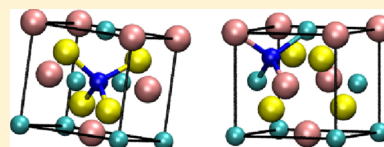
[§]Max Planck Institute for Chemical Physics of Solids, Nöthnitzer Straße 40, 01187 Dresden, Germany

^{||}CEA, DEN, Service de Recherches de Métallurgie Physique, UPSay, F-91191 Gif-sur-Yvette, France

[⊥]Wilhelm Büchner Hochschule, Ostendstraße 3, 64319 Pfungstadt, Germany

[▽]Department of Chemistry and Institute for Lightweight Design with Hybrid systems, University of Paderborn, Warburger Straße 100, 33098 Paderborn, Germany

ABSTRACT: We have studied the energetics, atomic, and electronic structure of Na and K point defects, as well as the (Na–Na), (K–K), and (Na–K) dumbbells in CuInSe_2 and CuIn_5Se_8 solar cell materials by hybrid functional calculations. We found that although Na and K behaves somewhat similar; there is a qualitative difference between the inclusion of Na and K impurities. Namely, Na will be mostly incorporated into CuInSe_2 and CuIn_5Se_8 either as an interstitial defect coordinated by cations, or two Na impurities will form (Na–Na) dumbbells in the Cu sublattice. In contrast to Na, K impurities are less likely to form interstitial defects. Instead, it is more preferable to accommodate K either as K_{Cu} substitutional defect, or to form (K–K) dumbbells on Cu substitution positions. Our data show that all (Na–Na), (Na–K), and (K–K) dumbbells can form in both CuInSe_2 and CuIn_5Se_8 . In the Cu-poor CuIn_5Se_8 material the pristine Cu vacancies act as the most stable sites where Na and K can be inserted. The formation energy of Na-related defects is generally lower than the corresponding K-related defects, which would mean that if a defect site is already occupied by Na, then it is less likely that K is able to substitute Na during the postdeposition treatment. Regarding the electronic structure of the materials, Na and K point defects located in the Cu sublattice do not create deep defect levels in the gap, so they are not detrimental for the solar cell. In contrast, Se-related substitutional defects introduce defect levels in the gap, which act as charge traps, leading to severe degradation of the device efficiency. However, the formation energy of these Se-related defects are high so that they should have a low concentration in the material.



INTRODUCTION

Cu(In,Ga)Se_2 (CIGSe) consisting of CuInSe_2 and CuGaSe_2 is widely used as light absorber layer in efficient and inexpensive thin film solar cells, which have produced maximum conversion efficiencies of up to 21.7%.^{1,2} In experimental studies, it has been shown that the incorporation of small amounts of Na and K with the concentration of around 0.1 atomic percent into the CIGSe layer increases the efficiency of the solar-cell devices.^{3,4} However, so far, the driving mechanism behind the benign effect of Na and K upon the efficiency of thin-film solar cells is not well understood, and their function is highly debated.

Considering the fact that in solar cells fabricated on an industrial scale, mainly soda-lime glass (SLG) is used as the substrate, the issue of Na and K impurities becomes even more important. Namely, SLG contains both Na and K in oxide form, and during the thin film deposition, these elements diffuse into the CIGSe absorber layer. The amount of K included in SLG, however, is less than Na.^{3,5} This is why the incorporation of Na into the absorber layer has been a very hot topic of scientific research,^{6–9} and was extensively studied since the work of Hedstroem et al.¹⁰ In contrast to Na, the diffusion and

incorporation of K into the absorber layer is a relatively new topic.^{3,11–13}

Solar cell devices based on CIGSe are manufactured with either a CdS ^{3,14,15} or a zinc oxysulfide (Zn(O,S)) buffer layer deposited between the CIGSe light absorber and the front contact.^{16,17} In the vicinity of the buffer layer, a heterojunction is formed between a p-type CIGSe and a Cu-poor CIGSe phase,¹⁸ which is widely accepted to be an ordered vacancy compound (OVC).^{19–21} Hence, the control over the incorporation of Na and K into the absorber layer is a crucial issue for increasing the efficiency of chalcopyrite thin-film solar cells. Na and K exhibit homologous behavior and have common chemical properties. This would suggest that they should have similar effects upon the atomic and electronic structure of the light absorber layer. Furthermore, taking into account the ionic radius of K^+ , which is larger than Na^+ , one would expect a lower diffusivity of K. The larger radius could also mean that K may not be able to occupy certain sites in the absorber layer.²²

Received: August 6, 2015

Revised: October 13, 2015

Published: October 14, 2015



To provide new insights from theoretical calculations on the structure and energetics of Na and K impurities in CIGSe light absorber, we study here the formation energies of K and Na defects in CuInSe_2 and CuIn_5Se_8 , which serve as models for the bulk CIGSe absorber and for the Cu-poor OVC compound, respectively. Through the results presented in this paper, we assess which lattice sites are more favorable to act as inclusion sites for Na and K, and which of these defects are detrimental for the efficiency of CIGSe solar cells. In addition to point defects related to Na and K, the formation of defect complexes like that of (Na–Na), (K–K), and (Na–K) dumbbells are also investigated.

■ COMPUTATIONAL METHODOLOGY

Computational Details. All calculations were carried out within the framework of density functional theory (DFT) as implemented in the VASP program package^{23,24} using the projector augmented-wave method.^{25,26} The wave functions were expanded up to a cutoff energy of 400 eV. For systems with an odd number of electrons, spin-polarized calculations have been performed. The exchange–correlation potential has been treated with the HSE06²⁷ hybrid functional. The parameter α , which determines the amount of Hartree–Fock exchange in the HSE06 calculations, has been set to 0.30.^{28–30} In the following, we will refer to this functional as HSE α . Instead of adjusting the fraction of exact exchange, other authors dealing with impurities in CuInSe_2 have preferred to tune the range separation parameter.^{31,32}

The crystal structure of the conventional tetragonal cells of bulk CuInSe_2 and the chalcopyrite polytype of CuIn_5Se_8 are shown in Figure 1. In this work, the calculations were carried

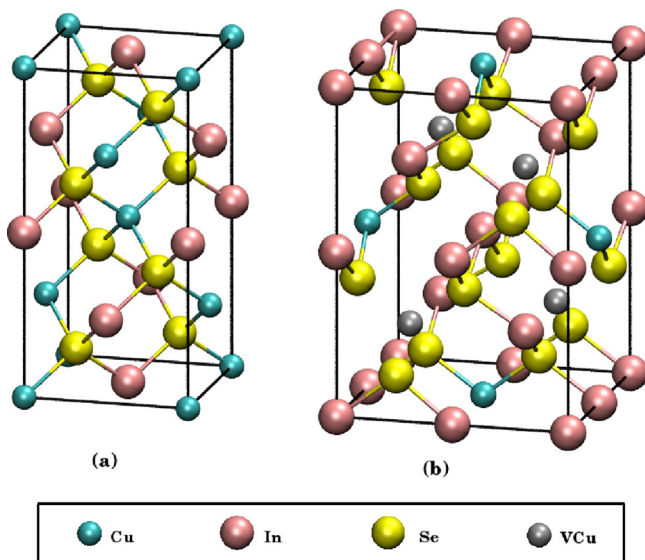


Figure 1. Crystal structure showing the conventional tetragonal unit cell of CuInSe_2 (a) and chalcopyrite polytype of CuIn_5Se_8 (b) ordered vacancy compound.

out for a 64-atom and 56-atom tetragonal supercells for CuInSe_2 and CuIn_5Se_8 , respectively. In order to estimate the dependency of the formation energies on the size of the supercell, we have performed test calculations on Na and K defects in large 216-atom supercells of CuInSe_2 , and we found that the formation energies were in the range of ± 0.1 eV compared to the 64-atom case. Hence, we expect that the data

presented here for the 64-atom and 56-atom supercells are qualitatively rather accurate, and using larger supercells would not change the results considerably. The Brillouin-zone integration was performed with a $2 \times 2 \times 2$ mesh of k-points. Throughout our study, we have used the theoretical equilibrium volume for the defect-free bulk CuInSe_2 and CuIn_5Se_8 . The optimized cell parameters and band gaps computed with HSE α are summarized in Table 1. In agreement with the experimental values, our results show that the calculated band gap of CuIn_5Se_8 is larger than that of the CuInSe_2 .

Table 1. Comparison between Experimentally Measured and Calculated Equilibrium Lattice Constants, a and c , Tetragonal Elongation, $\eta = c/a$, and Band Gaps, E_g , of CuInSe_2 and CuIn_5Se_8

	a (Å)	c (Å)	η	E_g (eV)	reference
CuInSe_2	11.68	11.75	1.006	1.04	current work
CuInSe_2	11.56	11.82	1.005	1.04	33, 34
CuIn_5Se_8	11.68	11.74	1.005	1.23	current work
CuIn_5Se_8	11.44	11.62	1.016	1.23	35, 36

Formation Energy Calculation. Supercell calculation is the most prevalent procedure to calculate the formation energy of impurities in bulk materials. In this method a defect α with charge state q is surrounded by a finite number of atoms of the bulk compound, and the whole structure is repeated periodically.³⁷ The dimension of the supercell has to be rather large to reduce the spurious interactions between the defect and its own periodic replicas.^{19,38} For charged defects, the long-range Coulomb interaction converges very slowly with the supercell size, so correction terms for finite-size effects are introduced. The formation energy of a defect or impurity α in charge state q is defined as

$$E_f[\alpha^q] = E_{\text{tot}}[\alpha^q] - E_{\text{tot}}[\text{pure}] + E_{\text{corr}}^q - \sum_i n_i \mu_i + q[E_{\text{VBM}} + \mu_e + \Delta v_{0/b}] \quad (1)$$

where $E_{\text{tot}}[\alpha^q]$ is the total energy of the supercell with the defect α in charge state q and $E_{\text{tot}}[\text{pure}]$ is the total energy of the equivalent defect-free bulk supercell. n_i represents the number of atoms of type i (host atoms or impurity atoms) that have been added to ($n_i > 0$) or removed from ($n_i < 0$) the bulk supercell when the defect or impurity is created. μ_i is the chemical potential of the elements in their native elemental state, that is, the energy of an atom from solid Cu (face-centered cubic), solid In (body-centered tetragonal), bulk Se (hexagonal phase with helical chains), and solid Na and K (body-centered cubic). These chemical potentials represent the reservoir's energy, with which atoms are being exchanged.³⁸ E_{VBM} is the valence band maximum (VBM) of the defect-free bulk and μ_e is the Fermi energy with respect to E_{VBM} . The range of μ_e is from zero (corresponding to a p -type material) to the value of the band gap (n -type material).

The formation energy appearing in eq 1 needs to be corrected due to the finite-size error. First, the total energy is corrected by $q\Delta v_{0/b}$, where $\Delta v_{0/b}$ is a term aligning the averaged electrostatic potential of the bulk and the supercell containing an associated neutral defect.⁴⁰ Next, the total energy is corrected by E_{corr}^q which accounts for the interaction of the charged defect. In this work, we used the approach proposed by Lany and Zunger⁴¹ to calculate E_{corr}^q .

RESULTS AND DISCUSSION

Defect Formation Energies. Na and K Point Defects in CuInSe₂. To study the energetics of point defect formation related to Na and K impurities, a Na or K atom was placed in a 64-atom supercell of CuInSe₂ either as an interstitial or as a substitutional defect. The atomic structure was fully relaxed with the HSE α functional for the charged and neutral defects. The calculated formation energies for different defects are summarized in Table 2 for the most stable charge state. Because

Table 2. Defect Formation Energy, in Electronvolts, Calculated with the HSE α Functional for Na and K Impurities in CuInSe₂ and CuIn₅Se₈ with the Electron Chemical Potential $\mu_e = 0$, That Is, Assuming a *p*-Type Material^b

defect	CuInSe ₂	CuIn ₅ Se ₈
Na _{Cu} ⁺	−1.16	−1.90
K _{Cu} ⁺	−0.49	−1.02
Na _{In} ⁰	0.96	1.49
K _{In} ⁰	1.67	1.89
Na _{Se} ⁺	0.66	0.29
K _{Se} ⁺	0.55	0.40
Na _{ac} ⁺	−1.17	−1.34
K _{ac} ⁺	0.48	−0.10
Na _{cc} ⁺	−1.25	−2.42 ^a
K _{cc} ⁺	−0.30	−1.67 ^a
Na _{V_{Cu}} ⁺		−2.43
K _{V_{Cu}} ⁺		−1.66
(Na–Na) _{Cu} ⁺	−2.29	−2.95
(Na–K) _{Cu} ⁺	−1.71	−2.12
(K–K) _{Cu} ⁺	−1.11	−2.17
(Na–Na) _{Cu} ²⁺	−2.50	−3.56
(Na–K) _{Cu} ²⁺	−1.93	−2.79
(K–K) _{Cu} ²⁺	−1.36	−2.83
(Na–Na) _{V_{Cu}} ²⁺		−4.09
(Na–K) _{V_{Cu}} ²⁺		−3.29
(K–K) _{V_{Cu}} ²⁺		−3.24
(Na–Na) _{V_{Cu}} ³⁺		−5.09
(Na–K) _{V_{Cu}} ³⁺		−3.99
(K–K) _{V_{Cu}} ³⁺		−4.04

^aRelaxed to V_{Cu} position ^bIn the CuIn₅Se₈ material, the V_{Cu} index refers to the pristine Cu vacancy site in the structure.

it is known from the experiment that the light absorber is a *p*-type material, in this work, all formation energies are reported for the scenario where the electron chemical potential μ_e is set at the VBM. Figure 2 shows the formation energy of various Na and K defects as a function of μ_e .

In full agreement with a previous work⁴² that was focused on Na impurities in CuInSe₂, we also found that among Cu, In, and Se substitutional sites, the Cu site is energetically the most favorable to host Na or K atoms. We found that for a *p*-type material where the chemical potential of the electron reservoir is at VBM, both for Na and K the positively charged Na_{Cu}⁺ and K_{Cu}⁺ defects are slightly more stable compared to the charge neutral Na_{Cu}⁰ and K_{Cu}⁰ defects. This is due to the larger electropositivity of Na and K with respect to Cu. However, we need to mention that the difference between the formation energies of neutral and +1 charged defects (about 0.08 eV) is comparable with the magnitude of the E_{corr}^q correction term. For Na_{Cu}⁰ and K_{Cu}⁰ substitutional defects, we have computed a

formation energy of −1.08 eV and −0.26 eV, respectively. The negative formation energies suggest that at low impurity concentration, such defects can be spontaneously formed. Considering the high formation energies of 0.96 and 1.67 eV calculated for Na_{In}⁰ and K_{In}⁰, respectively, creating substitutional defects in indium positions in CuInSe₂ is rather unlikely. Occupying selenium sites by Na or K atoms is also less likely, though the formation energies of 0.66 and 0.55 eV computed for Na_{Se}⁺ and K_{Se}⁺ are considerably lower in energy than the In substitutional defects. For substitutional defects on Cu and In positions, there is a qualitative difference between Na and K. Namely, the lower formation energies favor Na-related defects (on the order of 0.7 eV versus K). For comparison, on the Se site, the Na- and K-related substitutional defects are almost isoenergetic.

Besides the substitutional defects, we also studied the formation energy of Na or K defects in two different interstitial positions, where the impurity is either being coordinated to four Se anions (see Figure 3a), or four cations (two Cu and two In, Figure 3b). In Table 2 and throughout the text, these two interstitial positions are represented with the short hand notations *ac* and *cc*, respectively. Our results show, in agreement with ref 42, that the *cc* position is more favorable than the *ac* both for Na and K. The corresponding formation energy for the *cc* interstitial position is −1.25 and −0.30 eV for Na_{cc}⁺ and K_{cc}⁺ respectively, whereas the formation energies calculated at Na_{ac}⁺ and K_{ac}⁺ positions were −1.17 and +0.48 eV. We found that for Na, only the *cc* interstitial position is more favorable than all substitutional positions, and for K, it is energetically unfavorable to be situated in the *ac* interstitial position. From the perspective of the defect formation energy, our data indicates that there is a qualitative difference between Na and K also for the interstitial positions. Namely, for Na the energy difference of 0.08 eV between the *cc* and *ac* sites is negligible compared to the 0.78 eV for K. Thus, if Na and K were incorporated into CuInSe₂ as interstitials, Na could occupy both *cc* and *ac* sites, but K would sit predominantly on *cc* positions. Furthermore, by comparing the formation energies of the interstitial and substitutional defects, it is interesting to note that interstitial positions are thermodynamically more favorable than all substitutional positions for a Na atom. In contrast, this is not the case for K. Thus, our results indicate that for a heavily *p*-doped CuInSe₂ material (where $\mu_e = 0$ eV), Na point defects will be incorporated into the bulk CuInSe₂ light absorber material as interstitial defects. Above $\mu_e = 0.1$ eV the Na_{Cu} substitutional defect will become the most stable point defect. In contrast to Na, K will occupy substitutional positions in the Cu sublattice for the full range of μ_e that is, even under *n*-type conditions.

Na and K Dumbbells in CuInSe₂. In ref 42, it was shown that for Na impurities it is possible to form (Na–Na) dumbbells as substitutional defects in Cu sites of CuInSe₂. In light of the aforementioned results,⁴² we look here into the issue of whether (K–K) dumbbells can be formed in spite of the larger size of the K impurity. In addition, we have also investigated if mixed dumbbells can be created between Na and K. To clarify this question, we have carried out calculations on three different dumbbells, that is, (Na–Na), (Na–K), and (K–K) dumbbells located in a Cu substitutional site. Our study confirms that the formation of dumbbells is highly probable. We found that dumbbells formed by two Na atoms, or one Na and one K atom, or even by two K atoms, could occupy the Cu site, which is surprising due to the large size of these dumbbells.

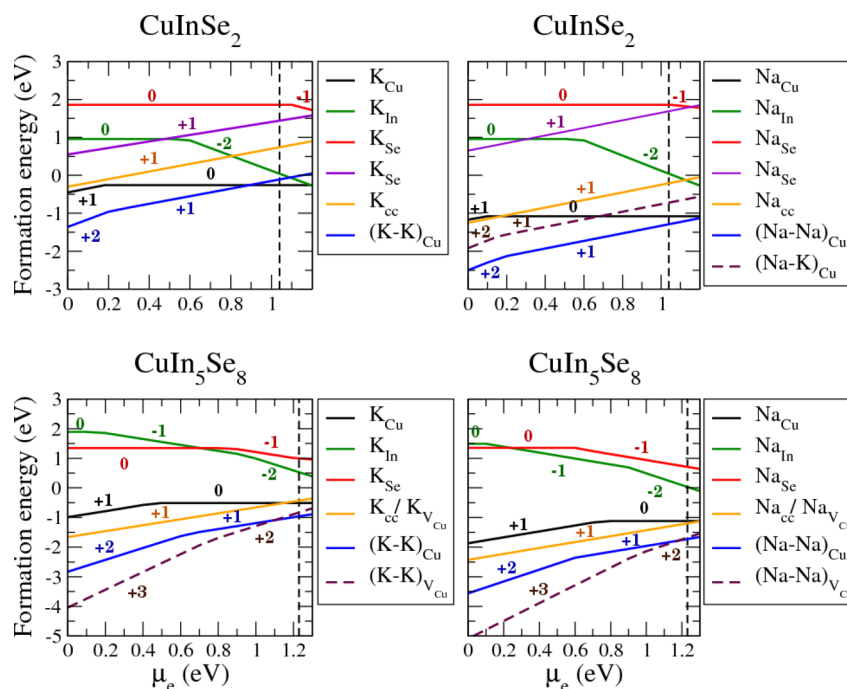


Figure 2. Formation energies of various Na and K defects in CuInSe_2 (top panel) and CuIn_5Se_8 (bottom panel) as a function of the electron chemical potential, where $\mu_e = 0$ corresponds to a p-type and $\mu_e = \text{CBM}$ (where CBM is the conduction band minimum) to an n-type material, respectively. The most stable charge state of the given defects is shown with positive and negative numbers. The horizontal dashed line shows the theoretically computed band gap for the bulk defect-free materials.

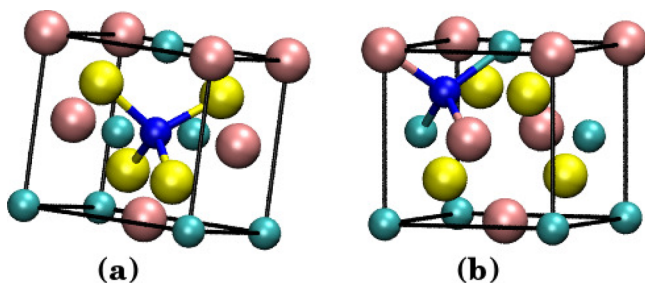


Figure 3. Position of the two different interstitial defects in CuInSe_2 . In subfigures a and b, the interstitial defect is tetrahedrally coordinated by four anions and by four cations, respectively. Na or K interstitials are shown as blue spheres, and the other atoms are presented using the same color scheme as in Figure 1. For clarity, only one-half of a CuInSe_2 conventional cell is shown.

The calculated formation energy of a $(\text{Na}-\text{Na})_{\text{Cu}}^{2+}$ dumbbell in a Cu substitutional position is -2.50 eV. Now, if we assume that in CuInSe_2 inserting two Na atoms in two distinct and spatially well separated cc interstitial position would result in a formation energy twice larger than a Na_{cc}^+ defect (i.e., -2.50 eV), then the formation of two separated interstitial defects competes with the formation of a dumbbell.

In contrast to Na, we found that for K atoms in CuInSe_2 , it will be always more preferable to form $(\text{K}-\text{K})_{\text{Cu}}^{2+}$ dumbbells with the formation energy of -1.36 eV, which is clearly more stable than having distinct K_{Cu}^+ or K_{cc}^+ defects. This binding energy computed for a $(\text{K}-\text{K})$ dumbbell compared to distinct K defects suggest that for the system, it is more favorable to cluster two K atoms together, probably due to reduced strain.

To check the accuracy of our results, we have recalculated the formation energy of the following defects in a 216-atom CuInSe_2 supercell: Na_{Cu}^+ , K_{Cu}^+ , Na_{cc}^+ , $(\text{Na}-\text{Na})_{\text{Cu}}^+$, $(\text{Na}-\text{K})_{\text{Cu}}^+$, and $(\text{K}-\text{K})_{\text{Cu}}^+$. The resulting formation energies were

subsequently -1.02 , -0.29 , -1.13 , -2.12 , -1.64 , and -1.10 eV, which shows that the energies presented in Table 2 are well converged even for the smaller 64-atom supercell.

Na and K Point Defects in CuIn_5Se_8 . After the investigation of the stoichiometric CuInSe_2 compound, we turn our attention here toward the Cu-poor CuIn_5Se_8 phase, which is representative of thin film solar cells grown under Cu-poor conditions and also to the OVC compounds found at the interface with the CdS buffer layer. The structure of CuIn_5Se_8 is obtained from CuInSe_2 by inserting a periodic arrangement of defect complexes formed by an indium antisite substituting copper (In_{Cu}) and two copper vacancies (referred as “pristine vacancies”⁴³), see Figure 1.

In the case of CuIn_5Se_8 , similarly to CuInSe_2 , the Cu site is the most favorable site within the substitutional positions for both Na and K atoms. However, Na_{Cu} and K_{Cu} substitutional defects in CuIn_5Se_8 are more likely to form compared with CuInSe_2 , despite the low Cu concentration in this Cu-poor phase. This is in agreement with the experimental finding that a KF treatment makes the absorber even more Cu poor.³

Under strongly doped p-type conditions, the formation of charge neutral Na_{In}^0 , K_{In}^0 , Na_{Se}^0 , and K_{Se}^0 defects are energetically very unfavorable, similarly to CuInSe_2 . In contrast to the CuInSe_2 stoichiometric compound, where the charge neutral Na_{In}^0 , K_{In}^0 , Na_{Se}^0 , and K_{Se}^0 defects are stable over a large range of the electron chemical potential μ_e in CuIn_5Se_8 and even in a p-type material, the $\text{Na}_{\text{In}}^{-1}$ and $\text{K}_{\text{In}}^{-1}$ defects become dominant once μ_e is larger than 0.1 eV (see Figure 2). Similarly, in CuIn_5Se_8 under n-type conditions the most stable charge state of the Se-related substitutional defects changes from charge neutral to $\text{Na}_{\text{Se}}^{-1}$ and $\text{K}_{\text{Se}}^{-1}$, whereas in CuInSe_2 the charge neutral state is the most stable for the whole range of μ_e .

The insertion of Na and K interstitials is energetically even more favorable in CuIn_5Se_8 than CuInSe_2 due to the presence

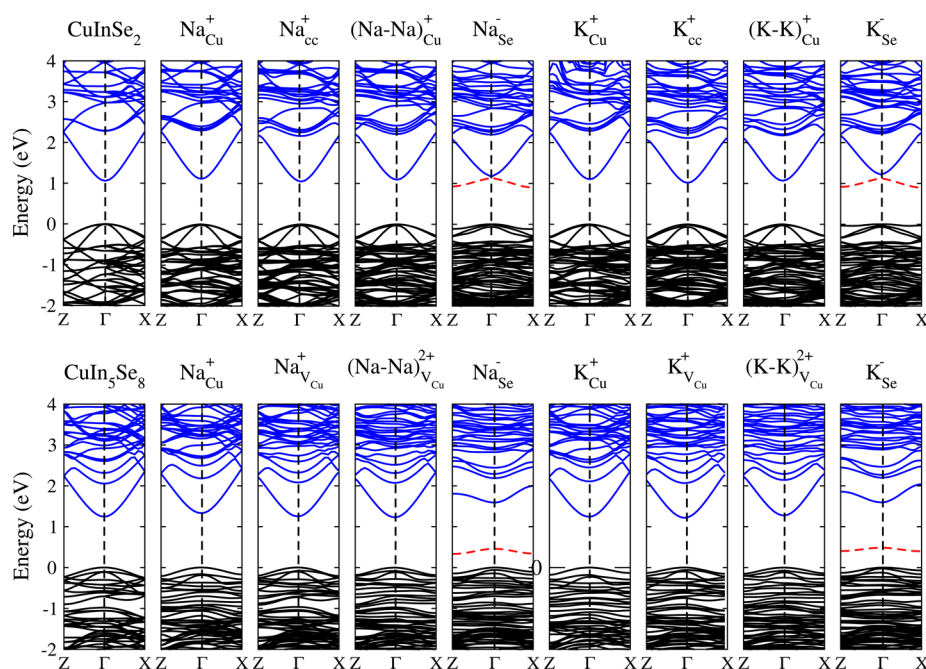


Figure 4. Band structure of the clean CuInSe_2 and CuIn_5Se_8 compounds and the systems with Na and K impurities. The top panel shows the calculated band structure for bulk CuInSe_2 , Na_{Cu}^+ , Na_{Cu}^+ , $(\text{Na-Na})_{\text{Cu}}^+$, Na_{Se}^- , K_{Cu}^+ , K_{Cu}^+ , $(\text{K-K})_{\text{Cu}}^+$, and K_{Se}^- defects in CuInSe_2 . The lower panel shows the band structure for CuIn_5Se_8 , Na_{Cu}^+ , Na_{Cu}^+ , $(\text{Na-Na})_{\text{Cu}}^{2+}$, Na_{Se}^- , K_{Cu}^+ , K_{Cu}^+ , $(\text{K-K})_{\text{Cu}}^{2+}$, and K_{Se}^- defects in CuIn_5Se_8 . The unoccupied and occupied levels are shown as black and blue lines, respectively, and red dashed lines represent the defect levels in the gap. The zero of energy is set to the bulk VBM.

of the two pristine Cu vacancies per formula unit, which make the accommodation of the interstitial defects easier in the structure. In fact, if we start the structural optimization from *cc* interstitial positions, then both of the Na and K interstitial atoms relax spontaneously to the pristine Cu vacancy site. By comparing the energetics of Na and K point defects in CuIn_5Se_8 , we found that energetically the most stable site for the inclusion of Na and K impurities is the pristine Cu defect site. The situation is similar but not identical to the case of Cd insertion,⁴³ similar to Na and K, Cd atoms prefer to occupy copper sites but due to difference in valance, Cd impurities induce a disordering of the pristine vacancy network.

Na and K Dumbbells in CuIn_5Se_8 . By inserting dumbbells into a Cu site as a substitutional defect or into a pristine vacant Cu site, we have also investigated the formation of dumbbells in the CuIn_5Se_8 material. We found that both Na and K atoms can enter in CuIn_5Se_8 in form of (Na–Na), (K–K), or mixed (Na–K) dumbbells. The formation of dumbbells in a pristine vacant Cu site is energetically more favorable than forming dumbbells as substitutional defects in a Cu position. This is not surprising considering that the CuIn_5Se_8 compound is already rather Cu poor compared to CuInSe_2 . Comparing the formation energies of the (Na–Na) dumbbell in a vacant Cu position with two Na in two pristine Cu positions reveals that the formation of two spatially separated Na point defects is as much likely as the formation of a Na dumbbell.

Band Structure and Charge Transition Levels of Na and K Defects. To assess the effect of Na and K impurities on the electronic structure of CuInSe_2 and CuIn_5Se_8 , first, we have calculated the band structure of the pure impurity-free compounds to serve as a reference. Next, we have evaluated the band structure (see Figure 4) of the most stable configurations for the Na and K impurities together with the unstable configurations where Na and K is located on Se substitutional positions. The band structures are calculated for

the most stable charge state across the band gap. We note that adding/removing one electron to/from the ground state of a system with large number of electrons change its band structure only slightly. This is due to the relaxation of all orbitals in the excited system. The larger band gap of CuIn_5Se_8 than CuInSe_2 is due to a periodic network of Cu vacancies, which decrease the contribution of Cu(d) orbitals at the top of the valence band of CuIn_5Se_8 , leading to a reduction of the Cu(d)–Se(p) interband repulsion. This lowers the VBM of CuIn_5Se_8 , resulting in a wider band gap.^{19,38}

In addition to the electronic band structures, we have also evaluated the thermodynamic charge transition levels of the various defects. The charge transition level $\epsilon_{\alpha}(q/q')$ was defined as the Fermi energy in eq 1 at which the formation energy of defect α with charge state q is equal to the formation energy of the given defect in another charge state q' . The higher ionization energy of deep levels reduce their contribution to the free charge carriers and acts like detrimental traps by acting as recombination centers. Recombination centers have roughly equal capture cross sections for both electrons and holes and are commonly stationed near the middle of the band gap. These levels are very detrimental in a photovoltaic cell, so the formation of such defects should be prevented because they reduce the cell's efficiency.

The calculated charge transition levels indicate that in CuInSe_2 , the Na_{Cu}^+ and K_{Cu}^+ defects induce extremely deep (0/+) transition levels, which are located 0.08 and 0.23 eV above the VBM, respectively. Thus, these defects do not act as recombination centers, and as a general result, we can conclude that Na and K point defects on Cu positions are not having a negative effect on the cell efficiency. In contrast, in CuIn_5Se_8 , they have (0/+) transition levels that are in the middle of the gap: for Na_{Cu}^+ , $E(0/+) = E_{\text{VBM}} + 0.78$ eV, and for K_{Cu}^+ , $E(0/+) = E_{\text{VBM}} + 0.50$ eV. This means that K_{Cu}^+ could act as a major electron trap, especially considering that due to the low

formation energy of this defect type, one would expect that K_{Cu} defects are abundant in the Cu-poor material. In agreement with our result, it has been shown previously by experiments that the incorporation of K during CIGSe growth at low process temperatures results in the formation of deep level defects.¹⁴ Two scenarios were suggested to explain these findings: either K impurities as point defects are directly responsible by creating these deep defect states, or K might impact the elemental interdiffusion, which leads to higher concentration of intrinsic defects. The investigation of such scenarios through experiments are rather cumbersome, and so far, no theoretical study has been carried out to shed new light on this issue.³⁹ According to our finding, the first scenario conforms to our calculations. However, we cannot either confirm or reject the second scenario without looking into the diffusion of the constituent atoms in CIGSe in the presence of Na and K.

The charge transition levels created by the (Na–Na) and (K–K) dumbbell in $CuInSe_2$ are located 0.18 and 0.21 eV above the VBM, respectively. This means that creating such dumbbells in the material is not destructive for the carrier transport. On the other hand, the formation of dumbbells by removing a Cu atom in $CuIn_5Se_8$ causes transition levels at 0.60 and 0.64 eV above the VBM for (Na–Na)_{Cu} and (K–K)_{Cu}, respectively. These levels are almost in the middle of the band gap, can act as recombination centers, and hinder the carrier transport. This is also true for the (K–K) dumbbell formed in the pristine Cu vacancy in $CuIn_5Se_8$; the transition level is located at 0.75 eV above the VBM. The (Na–Na)_{V_{Cu}} defect, however, causes a level 0.25 below the CBM that is harmless for the carrier transport.

In $CuInSe_2$, Na_{In} and K_{In} exhibit deep (–2/0) transition levels around $E_{VBM} + 0.60$ eV in the band gap, which correspond to a double acceptor level,⁴⁴ meaning that they undergo a charge transition from 0 directly to –2. Na and K in In site in $CuIn_5Se_8$ show a different behavior and induce two transition levels within the band gap, from 0 to –1 near the VBM, and from –1 to –2 near the CBM. Se-related substitutional defects for both Na and K induce a shallow level near the CBM in $CuInSe_2$ and a deeper level in $CuIn_5Se_8$. Such Se-related defect levels are clearly detrimental for the device efficiency; however, considering their high formation energies, these defects should have a low concentration in the CIGSe film. In general, we note that Na and K interstitial defects and dumbbells do not show any defect transition levels inside the band gap either in $CuInSe_2$ or in $CuIn_5Se_8$. Therefore, it can be concluded that Na and K in interstitial sites and also in the form of dumbbells do not create defects which would reduce the device efficiency.

SUMMARY AND CONCLUSIONS

In this paper, we have carried out hybrid functional computations on Na and K extrinsic defects investigating a wide gamut of substitutional and interstitial positions in $CuInSe_2$ and $CuIn_5Se_8$ solar cell materials. Our research reveals the most and least favorable insertion sites where Na and K can be situated in these compounds. Although Na and K behave rather similarly, we could still show that there is a qualitative difference between the preferred sites for Na and K impurities. Na is mostly incorporated either in form of interstitial defects coordinated by cations or into dumbbells in the Cu sublattice.

In comparison to Na, K does not form interstitial defects, but it prefers to assemble in the Cu sublattice to form (K–K) dumbbells. In $CuIn_5Se_8$, both Na and K prefers to occupy the pristine Cu vacancy sites either as point defects or by forming dumbbells. Because pristine Cu vacancy sites act as very stable inclusion sites for Na and K impurities, we expect that films grown under Cu-poor condition or containing Cu-poor OVC phases accommodate a larger concentration of Na and K compared to the stoichiometric $CuInSe_2$. For the K impurities, it is known experimentally that they improve the efficiency if the K-treatment of the cell is performed after the deposition of the film has finished, whereas if K is present in a high concentration during growth, that actually reduces the device characteristics.

In general, the formation energy of Na-related defects are lower than the corresponding K impurities in all studied sites. Considering the fact that Na is present most of the time in the CIGSe light absorber layer because of its diffusion from the glass substrate, and K is introduced during a post-deposition treatment, we think that it is highly unlikely that K will substitute Na from those sites that are already occupied by Na. Thus, if a higher K concentration would be desired, then making a Na-depleted substrate could be a precondition.

AUTHOR INFORMATION

Corresponding Author

*E-mail: mirhosse@cpfs.mpg.de.

Notes

The authors declare no competing financial interest.

ACKNOWLEDGMENTS

Financial support is gratefully acknowledged from the German *Bundesministerium für Wirtschaft und Energie* (BMWi) for the comCIGS II project (0325448C). E.Gh. would like to acknowledge IBM for the work proposal and for the computing resources.

REFERENCES

- (1) Jackson, P.; Hariskos, D.; Wuerz, R.; Kiowski, O.; Bauer, A.; Friedlmeier, T. M.; Powalla, M. Properties of $Cu(In,Ga)Se_2$ Solar Cells With New Record Efficiencies up to 21.7%. *Phys. Status Solidi RRL* **2015**, *9* (1), 28–31.
- (2) Green, M. A.; Emery, K.; Hishikawa, Y.; Warta, W.; Dunlop, E. D. Solar Cell Efficiency Tables (version 42). *Prog. Photovoltaics* **2013**, *21* (5), 827–837.
- (3) Chirilă, A.; Reinhard, P.; Pianezzi, F.; Bloesch, P.; Uhl, A. R.; Fella, C.; Kranz, L.; Keller, D.; Gretener, C.; Hagendorfer, H.; Jaeger, D.; Erni, R.; Nishiwaki, S.; Buecheler, S.; Tiwari, A. N. Potassium-Induced Surface Modification of $Cu(In,Ga)Se_2$ Thin Films For High-Efficiency Solar Cells. *Nat. Mater.* **2013**, *12*, 1107–1111.
- (4) Jackson, P.; Hariskos, D.; Lotter, E.; Paetel, S.; Wuerz, R.; Menner, R.; Wischmann, W.; Powalla, M. New World Record Efficiency For $Cu(In,Ga)Se_2$ Thin-Film Solar Cells Beyond 20%. *Prog. Photovoltaics* **2011**, *19* (7), 894–897.
- (5) Ishizuka, S.; Yamada, A.; Fons, P. J.; Shibata, H.; Niki, S. Interfacial Alkali Diffusion Control in Chalcopyrite Thin-Film Solar Cells. *ACS Appl. Mater. Interfaces* **2014**, *6* (16), 14123–14130.
- (6) Granata, J. E.; Sites, J. R.; Asher, S.; Matson, R. J. Quantitative Incorporation of Sodium in $CuInSe_2$ and $Cu(In,Ga)Se_2$ Photovoltaic Devices. *26th IEEE Photovoltaic Specialists Conf.* **1997**, 387–390.
- (7) Niles, D. W.; Ramanathan, K.; Hasoon, F.; Noufi, R.; Tielsch, B. J.; Fulghum, J. E. Na Impurity Chemistry in Photovoltaic CIGS Thin Films: Investigation With x-Ray Photoelectron Spectroscopy. *J. Vac. Sci. and Technol. A* **1997**, *15* (6), 3044–3049.

- (8) Braunger, D.; Hariskos, D.; Bilger, G.; Rau, U.; Schock, H. W. Influence of Sodium on the Growth of Polycrystalline Cu(In,Ga)Se₂ Thin Films. *Thin Solid Films* **2000**, 361–362 (0), 161–166.
- (9) Schroeder, D. J.; Rockett, A. A. Electronic Effects of Sodium in Epitaxial CuIn_{1-x}Ga_xSe₂. *J. Appl. Phys.* **1997**, 82 (10), 4982–4985.
- (10) Hedström, J.; Ohlsén, H.; Bodegård, M.; Kylner, A.; Stolt, L.; Hariskos, D.; Ruckh, M.; Schock, H. W. ZnO/CdS/Cu(In,Ga)Se₂ Thin Film Solar Cells With Improved Performance. *23rd IEEE Photovoltaic Specialists Conf.* **1993**, 364–371.
- (11) Reinhard, P.; Chirilă, A.; Blösch, P.; Pianezzi, F.; Nishiwaki, S.; Buecheler, S.; Tiwari, A. N. Review of Progress Toward 20% Efficiency Flexible CIGS Solar Cells and Manufacturing Issues of Solar Modules. *IEEE J. of Photovoltaics* **2013**, 3 (1), 572–580.
- (12) Wuerz, R.; Eicke, A.; Kessler, F.; Paetel, S.; Efimenko, S.; Schlegel, C. CIGS Thin-Film Solar Cells and Modules on Enamelled Steel Substrates. *Sol. Energy Mater. Sol. Cells* **2012**, 100, 132–137.
- (13) Reinhard, P.; Pianezzi, F.; Bissig, B.; Chirilă, A.; Blösch, P.; Nishiwaki, S.; Buecheler, S.; Tiwari, A. N. Cu(In,Ga)Se₂ Thin-Film Solar Cells and Modules- A Boost in Efficiency Due to Potassium. *IEEE J. of Photovoltaics* **2015**, 5 (2), 656–663.
- (14) Pianezzi, F.; Reinhard, P.; Chirilă, A.; Bissig, B.; Nishiwaki, S.; Buecheler, S.; Tiwari, A. N. Unveiling the Effects of Post-Deposition Treatment With Different Alkaline Elements on the Electronic Properties of CIGS Thin Film Solar Cells. *Phys. Chem. Chem. Phys.* **2014**, 16, 8843–8851.
- (15) Jackson, P.; Hariskos, D.; Wuerz, R.; Wischmann, W.; Powalla, M. Compositional Investigation of Potassium Doped Cu(In,Ga)Se₂ Solar Cells With Efficiencies Up to 20.8%. *Phys. Status Solidi RRL* **2014**, 8, 219–222.
- (16) Kobayashi, T.; Yamaguchi, H.; Nakada, T. Effects of Combined Heat and Light Soaking on Device Performance of Cu(In,Ga)Se₂ Solar Cells With ZnS(O,OH) Buffer Layer. *Prog. Photovoltaics* **2014**, 22, 115–121.
- (17) Nakamura, M.; Kouji, Y.; Chiba, Y.; Hakuma, H.; Kobayashi, T.; Nakada, T. Achievement of 19.7% Efficiency With a Small-Zized Cu(In,Ga) (SeS)₂ Solar Cells Prepared by Sulfurization After Selenizaion Process With Zn-Based Buffer. *39th IEEE PVSC* **2013**, 0849–0852.
- (18) Mönig, H.; Fischer, Ch.-H.; Caballero, R.; Kaufmann, C. A.; Allsop, N.; Gorgoi, M.; Klenk, R.; Schock, H.-W.; Lehmann, S.; Lux-Steiner, M. C.; Lauermann, I. Surface Cu depletion of Cu(In,Ga)Se₂ Films: An Investigation by Hard x-Ray Photoelectron Spectroscopy. *Acta Mater.* **2009**, 57, 3645–3651.
- (19) Zhang, S. B.; Wei, S. H.; Zunger, A.; Katayama-Yoshida, H. Defect Physics of the CuInSe₂ Chalcopyrite Semiconductor. *Phys. Rev. B: Condens. Matter Mater. Phys.* **1998**, 57, 9642–9656.
- (20) Zhang, S. B.; Wei, S. H.; Zunger, A. Stabilization of Ternary Compounds Via Ordered Arrays of Defect Pairs. *Phys. Rev. Lett.* **1997**, 78, 4059–4062.
- (21) Schmid, D.; Ruckh, m.; Grunwald, F.; Schock, H. W. Chalcopyrite/Defect Chalcopyrite Heterojunctions on the Basis of CuInSe₂. *J. Appl. Phys.* **1993**, 73 (6), 2902–2909.
- (22) Rudmann, D. *Effect of Sodium on Growth and Properties of Cu(In,Ga)Se₂ Thin Film Solar Cells*. Ph.D. Thesis, Swiss Federal Institute of Technology (ETH) Zuerich, 2004.
- (23) Kresse, G.; Furthmüller, J. Efficient Iterative Schemes For Ab-Initio Total-Energy Calculations Using a Plane-Wave Basis Set. *Phys. Rev. B: Condens. Matter Mater. Phys.* **1996**, 54, 11169–11186.
- (24) Kresse, G.; Furthmüller, J. Efficiency of Ab-Initio Total Energy Calculations For Metals and Semiconductors Using a Plane-Wave Basis Set. *Comput. Mater. Sci.* **1996**, 6 (1), 15–50.
- (25) Kresse, G.; Joubert, D. From Ultrasoft Pseudopotentials To the Projector Augmented-Wave Method. *Phys. Rev. B: Condens. Matter Mater. Phys.* **1999**, 59, 1758–1775.
- (26) Blöchl, P. E. Projector Augmented-Wave Method. *Phys. Rev. B: Condens. Matter Mater. Phys.* **1994**, 50, 17953–17979.
- (27) Heyd, J.; Scuseria, G. E.; Ernzerhof, M. Hybrid Functionals Based on Screened Coulomb Potential. *J. Chem. Phys.* **2003**, 118 (18), 8207–8215.
- (28) Kumagai, Y.; Soda, Y.; Oba, F.; Seko, A.; Tanaka, I. First-Principles Calculations of the Phase Diagrams and Band Gaps in CuInSe₂-CuGaSe₂ and CuInSe₂-CuAlSe₂ Pseudobinary Systems. *Phys. Rev. B: Condens. Matter Mater. Phys.* **2012**, 85, 033203.
- (29) Hinuma, Y.; Oba, F.; Kumagai, Y.; Tanaka, I. Ionization Potentials of (112) and (112) Facet Surfaces of CuInSe₂ and CuGaSe₂. *Phys. Rev. B: Condens. Matter Mater. Phys.* **2012**, 86, 245433.
- (30) Kiss, J.; Gruhn, T.; Roma, G.; Felser, C. Theoretical Study on the Diffusion Mechanism of Cd in the Cu-Poor Phase of CuInSe₂ Solar Cell Material. *J. Phys. Chem. C* **2013**, 117, 25933–25938.
- (31) Pohl, J.; Albe, K. Intrinsic Point Defects in CuInSe₂ and CuGaSe₂ As Seen Via Screened-Exchange Hybrid Density Functional Theory. *Phys. Rev. B: Condens. Matter Mater. Phys.* **2013**, 87, 245203–1–16.
- (32) Pohl, J.; Klein, A.; Albe, K. Role of Copper Interstitials In CuInSe₂: First-Principles Calculations. *Phys. Rev. B: Condens. Matter Mater. Phys.* **2011**, 84, 121201.
- (33) Paszkowicz, W.; Lewandowska, R.; Bacewicz, R. Rietveld Refinement for CuInSe₂ and CuIn₃Se₅. *J. Alloys Compd.* **2004**, 362 (1–2), 241–247.
- (34) Ariswan; El Haj Moussa, G.; Guastavino, F.; Llinares, C. Band Gap of CuInSe₂ Thin Films Fabricated by Flash Evaporation Determined From Transmission Data. *J. Mater. Sci. Lett.* **2002**, 21 (3), 215–217.
- (35) Durán, L.; Guerrero, C.; Hernández, E.; Delgado, J. M.; Contreras, J.; Wasim, S. M.; Durante Rincón, C. A. Structural, Optical and Electrical Properties of CuIn₃Se₈ and CuGa₃Se₈. *J. Phys. Chem. Solids* **2003**, 64 (9–10), 1907–1910.
- (36) Rincón, C.; Wasim, S. M.; Marín, G.; Márquez, R.; Nieves, L.; Pérez, G. S.; Medina, E. Temperature Dependence of the Optical Energy Gap and Urbach's Energy of CuIn₃Se₈. *J. Appl. Phys.* **2001**, 90 (9), 4423–4428.
- (37) Van de Walle, C. G.; Denteneer, P. J. H.; Bar-Yam, Y.; Pantelides, S. T. Theory of Hydrogen Diffusion and Reactions in Crystalline Silicon. *Phys. Rev. B: Condens. Matter Mater. Phys.* **1989**, 39, 10791–10808.
- (38) Van de Walle, C. G.; Neugebauer, J. First-Principles Calculations For Defects and Impurities: Applications to III-Nitrides. *J. Appl. Phys.* **2004**, 95 (8), 3851–3879.
- (39) Pianezzi, F. H. *Electronic Transport and Doping Mechanisms in Cu(In,Ga)Se₂ Thin Film Solar Cells*. Ph.D. thesis, Swiss Federal Institute of Technology (ETH) Zuerich, 2014.
- (40) Komsa, H.-P.; Rantala, T. T.; Pasquarello, A. Finite-Size Supercell Correction Schemes For Charged Defect Calculations. *Phys. Rev. B: Condens. Matter Mater. Phys.* **2012**, 86, 045112.
- (41) Lany, S.; Zunger, A. Assessment of Correction Methods For the Band-Gap Problem and For Finite-Size Effects in Supercell Defect Calculations: Case Studies For ZnO And GaAs. *Phys. Rev. B: Condens. Matter Mater. Phys.* **2008**, 78, 235104.
- (42) Oikkonen, L. E.; Ganchenkova, M. G.; Seitsonen, A. P.; Nieminen, R. M. Effect of Sodium Incorporation Into CuInSe₂ From First Principles. *J. Appl. Phys.* **2013**, 114 (8), 083503.
- (43) Kiss, J.; Gruhn, T.; Roma, G.; Felser, C. Theoretical Study On the Structure and Energetics of Cd Insertion and Cu Depletion Of CuIn₃Se₈. *J. Phys. Chem. C* **2013**, 117 (21), 10892–10900.
- (44) Han, D.; Sun, Y. Y.; Bang, J.; Zhang, Y. Y.; Sun, H.-B.; Li, X.-B.; Zhang, S. B. Deep Electron Traps and Origin of p-Type Conductivity in the Earth-Abundant Solar-Cell Material Cu₂ZnSnS₄. *Phys. Rev. B: Condens. Matter Mater. Phys.* **2013**, 87, 155206.